Desalination and Water Treatment
www.deswater.com

doi: 10.1080/19443994.2015.1130655

57 (2016) 22467–22479
October

Taylor & Francis
Taylor & Francis Group

Kinetics and thermodynamics of Pb sorption onto bentonite and poly(acrylic acid)/bentonite hybrid sorbent

Hamid R. Rafiei[a], Mehran Shirvani[a,*], Oladele A. Ogunseitan[b]

[a]*Department of Soil Science, College of Agriculture, Isfahan University of Technology, 84156-83111 Isfahan, Iran, Tel. +98 3133913471; email: rafiee.84@gmail.com (H.R. Rafiei), Tel. +98 3133913480; email: shirvani@cc.iut.ac.ir (M. Shirvani)*
[b]*Program in Public Health, Department of Population Health & Disease Prevention, University of California at Irvine, 92697-3957 Irvine, CA, USA, Tel. +1 949 824 6350, ext. 0611; email: Oladele.Ogunseitan@uci.edu*

Received 13 May 2015; Accepted 4 December 2015

ABSTRACT

In this work, bentonite (Bent) and poly(acrylic acid)–bentonite (PAA–Bent) hybrid were applied for the removal of Lead (Pb) from aqueous solutions. Sorption experiments were conducted under batch condition at different times, Pb concentrations, and temperatures. Equilibrium studies showed that Pb sorption data on PAA–Bent followed the Langmuir model. Both capacity and affinity of PAA–Bent and Bent for Pb retention increased with rising temperature. Maximum capacity (q_m) of PAA–Bent for Pb sorption was 91.88 mg g^{-1} at 15°C which increased to 96.13 mg g^{-1} at 50°C. For the Bent sample, the q_m values were 52.31 and 82.51 mg g^{-1}, respectively, at 15 and 50°C. The Langmuir Pb sorption affinity parameter (K_L) was increased from 0.12 to 2.25 L mg^{-1} for PAA–Bent and from 0.009 to 1.19 L mg^{-1} for Bent, as temperature rose from 15 to 50°C. Pseudo-first and pseudo-second-order kinetic models could best describe the time-dependent Pb sorption data by the PAA–Bent which occurred at a fast rate approaching equilibrium within ~30–60 min. For the Bent sample, the Elovich model was the best fitted model to the Pb sorption data. Calculation of thermodynamic parameters including Gibbs free energy changes (ΔG° = −20.07 to −40.63 kJ mol^{-1}), enthalpy change (ΔH° = 146.359 kJ mol^{-1}), and entropy change (ΔS° = 578.42 J mol^{-1} K^{-1}) showed that Pb sorption on the PAA–Bent is more spontaneous, endothermic, and favored as compared to Pb sorption process on the Bent with ΔG°= –19.51 to −30.44 kJ mol^{-1}, ΔH° = 70.02 kJ mol^{-1} and ΔS° = 310.94 J mol^{-1} K^{-1}. In conclusion, the PAA–Bent hybrid sorbent can be considered as a suitable candidate for the removal of Pb from aqueous solutions.

Keywords: Montmorillonite; Organo-clay; Lead; Adsorption

1. Introduction

Environmental contamination with toxic metals has become a global concern that threatens human health [1,2]. Lead (Pb) has been recognized as one of the most common toxic heavy metals, due to its wide application in many industries [3]. Wastewater processing from lead–acid batteries, paints, phosphate fertilizers, electronics, combustion of fossil fuels, forest fires, mining activities, automobile emissions, and corrosion of Pb-containing piping material are the major sources releasing Pb into the environment [1,2]. Lead

*Corresponding author.

poisoning typically results from the ingestion of contaminated food or water and can cause a variety of symptoms, especially in children, depending on the duration of Pb exposure [2,3]. Damage to liver and kidney, anemia, mental retardation, depression, increase in blood pressure, nausea, infertility, abdominal pain, fatigue, problems with sleep, headaches, stupor, slurred speech, and loss of coordination are some reported symptoms of chronic Pb poisoning [2,3]. In 1991, the US Centers for Disease Control and Prevention (CDC) established an acceptable blood lead level (BLL) of 10 μg/dL for children, but recently, the CDC reduced the threshold to 5 μg/dL [4].

Various technologies such as chemical precipitation, membrane separation, advanced oxidation process, electrochemical technique, and adsorption procedures have been developed for Pb(II) removal from wastewaters [5]. Among these methods, adsorption has some advantages, such as flexibility in design and operation, low cost, and producing superior effluent suitable for reuse without other pollutants [5,6]. Activated carbon is the most commonly used adsorbent due to its large surface area and high thermal stability, but the high cost, low adsorption efficiency and difficulties in the separation of powdered activated carbon from wastewater for regeneration limit its large-scale application as an adsorbent [7,8]. To date, different types of natural and synthetic sorbents including clay minerals (e.g. bentonite, palygorskite, and kaolinite) [9–11], multi-walled carbon nanotubes [12], mercapto-functionalized sepiolite [13], zeolite–nanoscale zero-valent iron composite [14], 8-hydroxy quinoline-immobilized bentonite [15], N-methylimidazole-modified palygorskite [16], as well as various biosorbents [17,18], and polymers [19–21] have been used for removing of metals from aqueous solutions.

Adsorption using innovative clay/polymer hybrid materials is regarded as one of the most effective methods to remove heavy metals from aqueous solutions, because these hybrids possess lots of functional groups and unique network structure [7,8,22–26]. Clays represent promising support materials for polymers due to their mechanical and chemical stability, low cost, abundant availability, and non-toxicity to organisms [7,24]. For example, Zhao et al. [23] reported the application of bentonite–polyacrylamide composite for the removal of copper(II) from aqueous solutions. Polymer-supported nanosized hydrated Fe (III) oxides were also shown to efficiently remove Pb (II), Cd(II), and Cu(II) from drinking water [24]. Nanohydroxyapatite–alginate composite [25] and carboxymethyl cellulose-g-poly (acrylic acid)/attapulgite hydrogel composites [8] are among other organic–inorganic hybrid materials used for Pb(II) adsorption from aqueous solutions. The bare clay and polymer particles are easily aggregated or coagulated in aqueous solutions, limiting their practical usage. This limitation can be minimized by the use of insoluble clay–polymer composites [8,26]. Furthermore, the clay fillers disperse within the polymer and increase the surface area for sorption since agglomeration is largely limited [22].

Possessing many polar carboxyl groups in its structure, poly(acrylic acid) (PAA) has shown a great ability to form strong complexes with metal ions in solution [7,8,27–29]. The high water solubility and weak structural stability of PAA, however, hinders application of this polymer to remove heavy metal ions from wastewater. Combining this polymer with clay minerals can help to overcome these limitations. He et al. [30] produced a kind of PAA/bentonite composite by *in situ* polymerization of acrylic acid monomers in bentonite (Bent) interlayer spaces, and successfully utilized the composite to remove lead(II) ions from solutions. In our previous work [31] we also prepared and characterized a new hybrid sorbent by grafting of PAA into the Bent galleries and studied equilibrium parameters of Pb sorption by the prepared sorbent. In the present work, the effects of contact time, initial concentration, and temperature on Pb sorption by the hybrid sorbent were investigated.

2. Experimental

2.1. Materials

The natural Bent was obtained from Mehredjan mine (33° 36′ 7″ N, 55° 10′ 4″ E), Isfahan, Iran. The chemical constituent of the Bent was analyzed by XRF and given in Table 1. The cation exchange capacity (CEC) of the clay, determined by Na-acetate method [32], was 66 $cmol^{+}\,kg^{-1}$. A stock solution of Pb (2,000 mg L^{-1}) was prepared by dissolving required amount of $Pb(NO_3)_2$ in 0.01 M $CaCl_2$ solution as background electrolyte. The stock solution was then diluted to the various concentrations between 50 and 1,200 mg Pb L^{-1}. N-Cetyltrimethylammonium (CTA) bromide (purity > 99%) with chemical formula of $C_{16}H_{33}N(CH_3)_3Br$ from Merck and PAA (MWca. 2000) from Sigma–Aldrich were used in preparation of the nanocomposite. All other chemicals used in this study were of analytical grade and all solutions were prepared with distilled water.

2.2. Preparation of PAA–Bent nanocomposite

Synthesis of surfactant-modified Bent (organo-clay) was carried out using CTA as intercalating species

Table 1
Chemical composition of natural bentonite obtained from X-ray fluorescence spectroscopy

Component	SiO_2	Al_2O_3	Fe_2O_3	MgO	CaO	K_2O	TiO_2	Na_2O	LOI[a]
Weight (%)	66.37	13.24	2.04	2.37	1.79	0.51	0.13	1.69	10.83

[a]Loss of ignition.

according to the following procedure. Twenty grams of natural Bent was mixed with 300 mL of distilled water and 6 mL of 0.01 M HCl. The mixture was subsequently heated to 70˚C for 2 h. An amount of CTA equivalent to 2CEC of the Bent was dispersed into the Bent suspension and stirred vigorously for 12 h at 70˚C. The mixture was then centrifuged and washed several times with hot distilled water until no bromide ion was detected by a 0.01 M $AgNO_3$ solution. The CTA-modified Bent was dried in an oven at 80˚C for 24 h and ground to 270 mesh (0.05 mm).

For the synthesis of PAA–organo/Bent hybrid, 10 g of surfactant-modified Bent was dispersed in 200 mL of phosphate buffer solution (pH 4.0), cooled to 4˚C, and sonicated for 10 min at 20 kHz frequency and rated power of 120 W. Then, 200 mL of a 5% PAA aqueous solution was added to the reaction flask and sonication was continued for 30 min at 4˚C. The mixture was then stirred at 60˚C for 3 h, centrifuged at 5,000 rpm for 20 min, and the sediment was dried in oven at 70˚C for 24 h. The dried sample was subsequently ground and particles smaller than 0.05 mm was used in the batch Pb(II) sorption studies.

2.3. Characterization of the sorbents

Infrared spectra of the sorbents were recorded using a JASCO FT-IR 460 spectrometer in range of 400–4,000 cm^{-1}. In order to characterize the initial material, a spectrum of pure CTA surfactant and PAA were also recorded. X-ray diffraction (XRD) analyses of the powdered samples were performed using a Philips PANalytical X'pert high score diffractometer with Cu Kα radiation, running at 40 kV and 40 mA, over the 2θ range of 2˚–40˚. The total carbon content in natural and modified bentonites was determined by a Skalar Primacs^{SLC} carbon analyzer. Electron micrographs of the gold-coated samples were taken using a scanning electronic microscope (SEM) (VEGA/TESCAN model).

2.4. Lead sorption experiments

Lead sorption experiments were conducted in batch mode under natural pH conditions with background electrolyte concentration of 0.01 mol L^{-1} $CaCl_2$. The initial pH value of the Pb solutions ranged from 5.69 to 4.93 depending on the Pb concentration. Isothermal experiments were conducted at different temperatures (15–50˚C) by mixing 0.15 g subsamples of each sorbent with 20 mL of aqueous solutions with increasing Pb concentration from 50 to 1,200 mg L^{-1} in 50 mL polyethylene centrifuge tubes. The mixtures were shaken in a thermostatic mechanical shaker at 180 rpm. After shaking for 24 h, the solid and liquid phases were separated by centrifugation at 2,500 rpm for 10 min and the residual Pb concentrations in the supernatants were determined using a Perkin Elmer AAnalyst200 atomic absorption spectrometer (AAS) at a wavelength of 283.3 nm. Equilibrium pH values in the supernatants were also measured. Sorption of Pb for each sample was calculated through the following equation:

$$q_e = \frac{(C_0 - C_e)V}{m} \quad (1)$$

where q_e refers to the amount of Pb sorbed (mg g^{-1}), C_0 and C_e represent the initial and equilibrium Pb concentration (mg L^{-1}), respectively, V is the volume of the aqueous solution (L), and m is the mass of dry sorbent (g). The Pb sorption percentage, R (%), after a certain period of time was calculated from the difference of initial and final Pb concentrations using the following equation:

$$R\,(\%) = \frac{C_0 - C_t}{C_0} \times 100 \quad (2)$$

where C_0 and C_t are the initial and final Pb concentrations (mg L^{-1}), respectively. All Pb removal experiments were conducted in triplicates. Blank experiments, without the addition of sorbents, were also considered to ensure that the decrease of Pb concentration was actually caused by the sorption onto the sorbents, rather than the tube wall.

The experimental data were fitted to the Langmuir and Freundlich isotherm equations. The non-linear equation of the Langmuir isotherm model is [33]:

$$q_e = \frac{q_m K_L C_e}{1 + K_L C_e} \quad (3)$$

where q_m is the maximum Pb sorption capacity (mg g^{-1}) and K_L (L mg^{-1}) is the affinity of Pb ions to the sorption sites. To determine if adsorption process is favorable, a dimensionless constant named separation factor or equilibrium parameter, which is defined as below was calculated [16]:

$$R_L = \frac{1}{1 + K_L C_0} \quad (4)$$

where K_L is the Langmuir constant and C_0 is the highest initial metal concentration (mg L^{-1}). If R_L values lie between 0 and 1, the adsorption is favorable [16].

The non-linear equation of the Freundlich sorption model is as follows [33]:

$$q_e = K_F C_e^N \quad (5)$$

where K_F and N are the Freundlich constants indicating Pb sorption capacity and intensity, respectively.

Thermodynamic parameters for Pb sorption including changes in Gibbs free energy (ΔG°), enthalpy (ΔH°), and entropy (ΔS°) were calculated using the following equations [34,35]:

$$\Delta G^\circ = -RT \ln K_d \quad (6)$$

where R is the universal gas constant (8.314 J mol^{-1} K^{-1}), T is the temperature (K), and K_d is the distribution coefficient of the solute between the adsorbent and the solution in equilibrium. The K_d value was calculated using following equation:

$$K_d = \frac{q_e}{C_e} \quad (7)$$

where C_e and q_e were defined earlier. The enthalpy change (ΔH°) and entropy change (ΔS°) were then estimated from the slope and intercept of plots of $\ln K_d$ vs. $1/T$, respectively, according to the following equation [34,35]:

$$\ln K_d = \frac{\Delta S^\circ}{R} - \frac{\Delta H^\circ}{RT} \quad (8)$$

For the kinetic studies, 0.15 g subsamples of each sorbent were mixed with 20 mL of solutions containing 400 or 800 mg L^{-1} of Pb. A series of such conical centrifuge test tubes were then shaken at a constant speed of 180 rpm. Samples were collected at predetermined time intervals (10, 30, 60, 120, 240, 480, 960, and 1,440 min), centrifuged and the supernatants were analyzed for Pb concentration using the AAS.

Four most commonly used kinetic models i.e. pseudo-first-order, pseudo-second-order, intraparticle diffusion, and Elovich models [15,33,36], were used to describe the experimental data using non-linear regression. The uniformity between the experimental data and model-predicted values was expressed by determination coefficients (R^2) values. The pseudo-first-order model is expressed in Eq. (9):

$$q_t = q_e(1 - e^{-k_1 t}) \quad (9)$$

where q_t and q_e are the amount of Pb sorbed (mg g^{-1}) at time t (min) and at equilibrium, respectively, and k_1 (min^{-1}) is the rate constant of the pseudo-first-order adsorption process.

The pseudo-second-order model can be described in Eq. (10):

$$q_t = \frac{k_2 q_e^2 t}{1 + k_2 q_e t} \quad (10)$$

where k_2 is the constant of pseudo-second-order rate (g mg^{-1} min^{-1}). The initial sorption rate "h" (mg g^{-1} min^{-1}), can also be calculated using the pseudo-second-order parameters as follows:

$$h = k_2 q_e^2 \quad (11)$$

The Elovich kinetic equation is often used to interpret the kinetics of chemisorption on highly heterogeneous sorbents. It can be expressed as Eq. (12):

$$q_t = \frac{1}{\beta}\ln(\alpha\beta) + \frac{1}{\beta}\ln t \quad (12)$$

where α and β are constants [36].

The intraparticle diffusion equation can be written as follows:

$$q_t = k_i t^{0.5} + I \quad (13)$$

where I is the intercept and k_i is the intraparticle diffusion rate constant (mg g^{-1} $min^{-1/2}$).

3. Results and discussion

3.1. Sorbents characteristics

The XRD patterns of the Bent, PAA–Bent and CTA–Bent are presented in Fig. 1. Reflection at $2\theta = 7.14^{\circ}$ (basal spacing of 1.2 nm) revealed in the XRD pattern of Bent indicated montmorillonite as a major phase. Minor phases were quartz ($2\theta = 26.6^{\circ}$) and cristobalite ($2\theta = 21.8^{\circ}$). The structural changes of montmorillonite are mainly reflected in the shifting of d_{001} peak towards the lower values of 2θ [37]. The basal spacing of the CTA–Bent and PAA–Bent increased to 3.55 and 3.88 nm, respectively, indicating intercalation of the surfactant and polymer into the interlayer spaces of Bent and formation of the intercalated nanostructure. This d-value is a result of the orientation of surfactant chains in the interlayers of the clay with a paraffinic or pseudo-trilayer arrangement [38,39]. Surfactants such as alkyl ammonium compounds mainly enlarge the interlayer spacing of clays and facilitate the penetration of polymers into the clay galleries during the preparation of the polymer/clay composites [38].

The FT-IR spectra of Bent, CTA–Bent, PAA–Bent, surfactant (CTA) and polymer (PAA) are shown in Fig. 2 and the spectral bands are summarized in Table 2. The FT-IR spectra of the modified bentonites were different from that of the Bent. The band at 1,637.2 cm^{-1} is related to the bending vibration of hydroxyl groups from water molecules [40,41]. FT-IR spectrum of PAA shows stretching vibrations of C=O group (carboxyl or carbonyl) at 1,647.8 cm^{-1} [42,43].

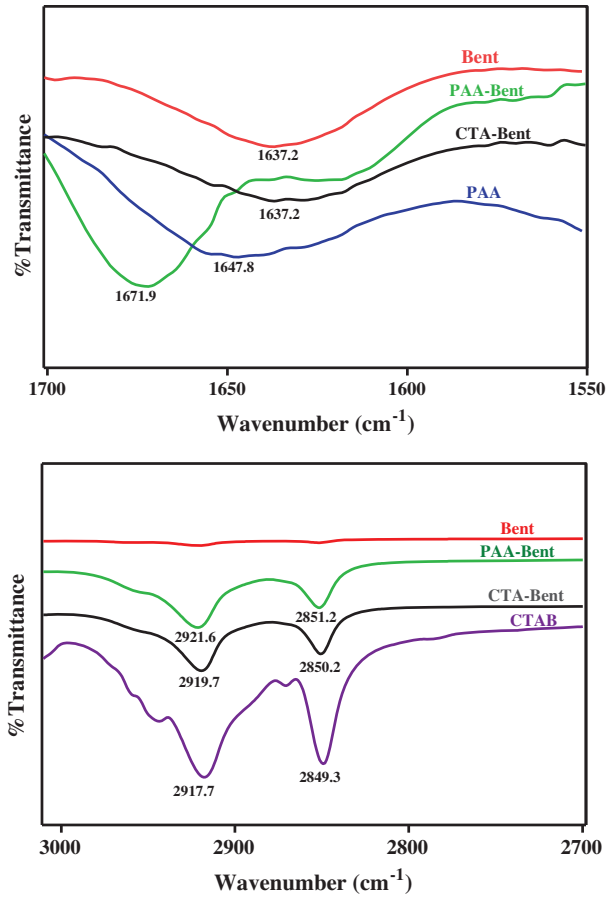

Fig. 2. FT-IR spectra of bentonite (Bent), cetyltrimethylammonium bromide (CTAB), polyacrylic acid (PAA), CTA–Bent, and PAA–Bent.

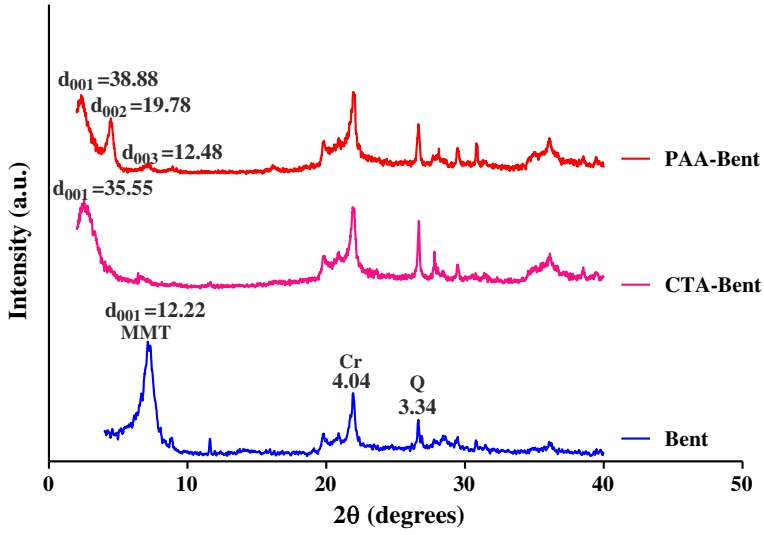

Fig. 1. XRD diffractograms of bentonite (Bent), organo-bentonite (CTA-Bent), and polyacrylic acid organo–bentonite (PAA-Bent).

Table 2
FT-IR vibration band positions and their assignments for bentonite (Bent), cetyltrimethylammonium bromide (CTAB), polyacrylic acid (PAA), CTA–Bent, and PAA–Bent

Assignment	Band position (cm^{-1})				
	Bent	CTAB	CTA-Bent	PAA	PAA-Bent
H–O–H bending vibration	1,637.27	–	1,637.27	–	–
C=O stretching vibration	–	–	–	1,647.87	1,671.98
Symmetric C–H stretching vibration	–	2,849.31	2,850.27	–	2,851.24
Asymmetric C–H stretching vibration	–	2,917.77	2,919.7	–	2,921.63
H–O–H stretching vibration (for H_2O)	3,435.56	–	3,434.6	–	3,433.64

This characteristic band was shifted to higher frequencies (1,671.9 cm^{-1}) after the polymer was combined with the clay which can be related to the interactions between the C=O groups and the clay surfaces [44]. New absorption bands were detected at 2,850.2 and 2,919.7 cm^{-1} in the spectrum of CTA–Bent, which were assigned to stretching vibrations of C–H bond in $–CH_2$ and in $–CH_3$ group of the aliphatic chain of the CTA surfactant [40,45]. Additionally, the bending vibration of the methyl groups can be observed at 1,468.5 cm^{-1}, verifying the intercalation of surfactant molecules between the silicate layers [44,46].

The experimental values of organic carbon content of the Bent and the CTA–Bent were 0.05 and 27.81%, respectively. Hence, the organic carbon in the CTA–Bent sample was almost entirely derived from the exchanged organic cations. Surfactant loading was fairly close to 185% of the CEC of the clay. The OC content of the PAA–Bent was 29.86%, suggesting that the PAA reacted successfully with the CTA–Bent. The morphologies of CTA–Bent and PAA–Bent are represented in Fig. 3, showing layered structure and nanosize scale.

3.2. Lead sorption kinetics

Fig. 4 shows the removal percentage of Pb from aqueous solution by Bent and PAA–Bent hybrid as a function of contact time at initial Pb concentration of 400 and 800 mg L^{-1}. For both Pb concentrations, the initial sorption rate was high because sufficient adsorption sites were available for Pb ions to interact with easily. However, the number of unoccupied sites decreases with time, slowing down the Pb sorption reaction [47]. Sorption of Pb on the PAA-Bent was very fast at the lower Pb concentration (C_0 = 400 mg L^{-1}) where more than 99.4% of the Pb sorption took place within the first 30 min, suggesting high complexation affinity between Pb ions and reactive functional groups on the surface of PAA–Bent. Lead sorption process on the Bent, however, approached equilibrium beyond the 1,440 min applied in this study for the sorption tests. Maximum Pb removal from solution by the Bent was only 63%.

At initial Pb concentration of 800 mg L^{-1}, the percentage of Pb sorbed from the solution by the PAA–Bent was 74.7% compared with the 51.8% sorbed

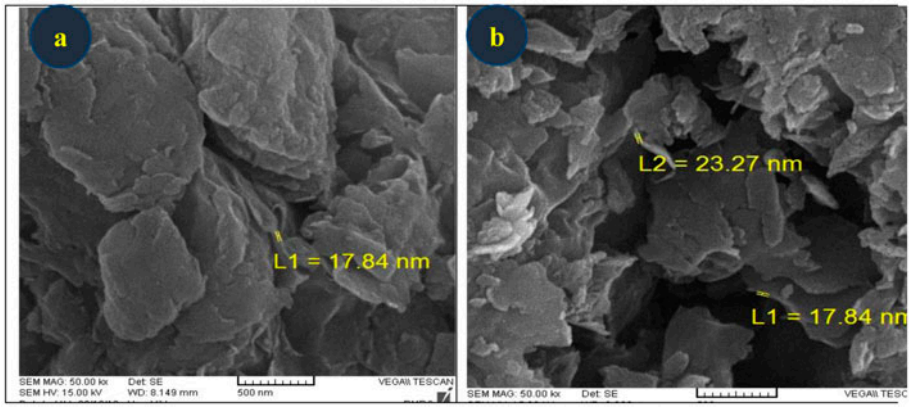

Fig. 3. SEM images of PAA–Bent (a) and CTA–Bent (b).

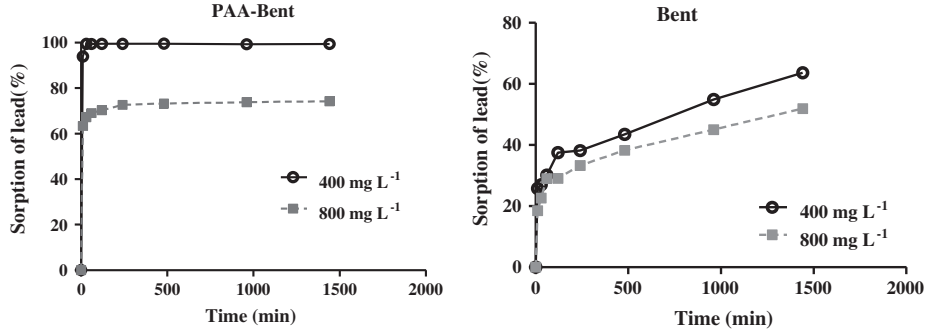

Fig. 4. Effects of initial concentration and time on lead adsorption percentage onto PAA–Bent and Bent (sorbent dose = 0.15 g; T = 25°C).

by the Bent (Fig. 4). At higher Pb concentrations, more Pb ions were left unadsorbed in solution due to the saturation of binding sites [11,47]. The time required to reach equilibrium increased with increasing the initial Pb concentration. For instance, as the Pb concentration increased from 400 to 800 mg L^{-1}, the equilibrium time for Pb sorption by the PAA–Bent nanocomposite increased from ~30 to ~60 min. However, equilibrium was not attained for Pb sorption by Bent within the experimental timescale applied in this study.

The Pb sorption kinetic parameters derived from various models are shown in Table 3. It is obvious that the sorption kinetics of Pb onto PAA–Bent follows the pseudo-second-order and pseudo-first order kinetic models better than the Elovich and intraparticle diffusion models (Table 3, Fig. 5), suggesting that the sorption process is probably controlled by

Table 3
Kinetic model constants and correlation coefficients for Pb sorption onto Bent and PAA–Bent at various initial Pb concentrations

	Sorbents			
	Bent		PAA-Bent	
Kinetic parameters	400 mg Pb L^{-1}	800 mg Pb L^{-1}	400 mg Pb L^{-1}	800 mg Pb L^{-1}
$q_{e(exp)}$ (mg g^{-1})	33.51	57.08	52.33	81.58
Pseudo-first-order				
q_e (mg g^{-1})	25.86	43.87	52.68	78.82
k_1 (min^{-1})	0.0271	0.0291	0.291	0.293
R^2	0.739	0.788	0.998	0.986
Pseudo-second-order				
q_e (mg g^{-1})	27.58	47.98	53.48	80.58
k_2 (g mg^{-1} min^{-1})	0.0014	0.0007	0.0156	0.0078
h (mg g^{-1} min^{-1})	1.07	1.79	44.61	50.97
R^2	0.824	0.878	0.988	0.992
Intra-particle diffusion				
k_i (mg g^{-1} $min^{-1/2}$)	0.696	1.177	0.575	0.998
I	8.01	15.52	37.96	55.14
R^2	0.865	0.823	0.183	0.267
Elovich model				
α (mg g^{-1} min^{-1})	18.36	30.66	786.0	1245.0
β (g mg^{-1})	0.316	0.179	0.199	0.132
R^2	0.922	0.950	0.712	0.776

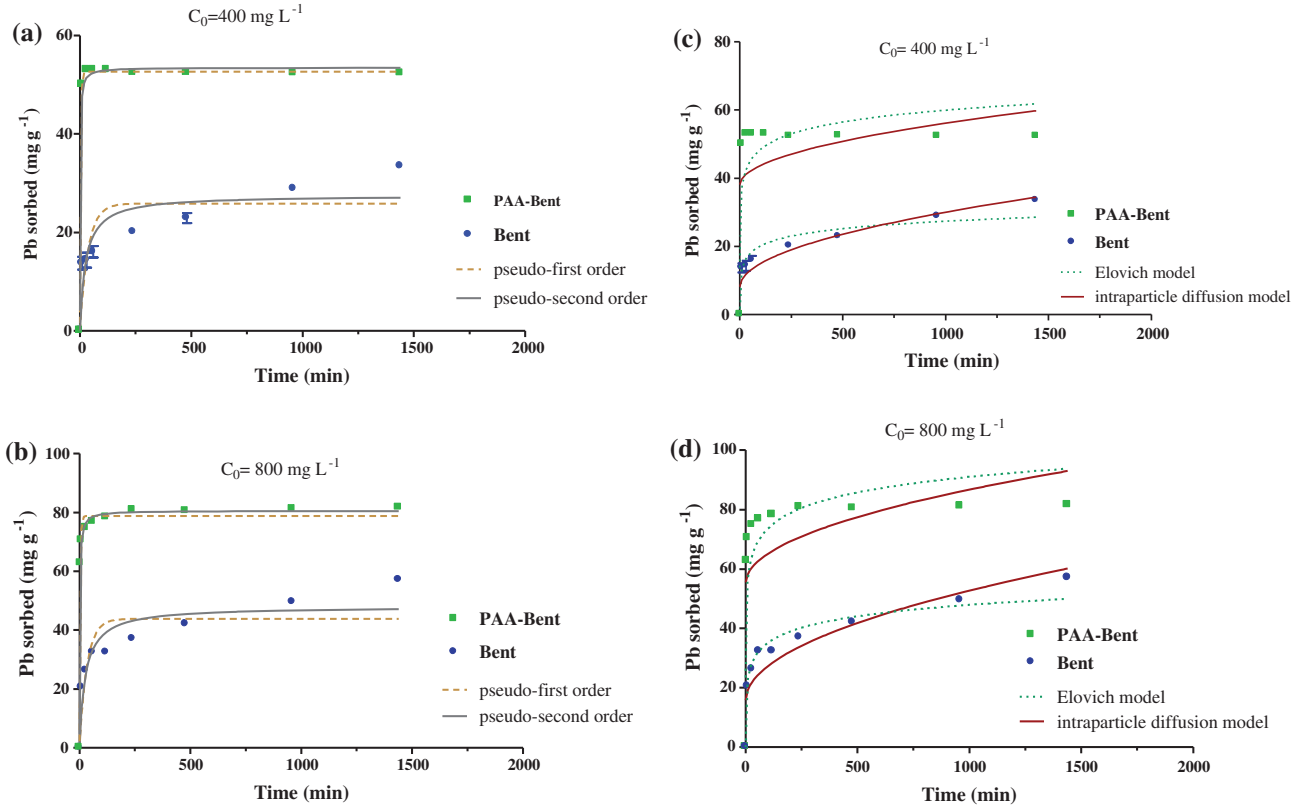

Fig. 5. Different sorption kinetic models applied to Pb sorption data by PAA–Bent and Bent at various initial concentrations.

chemisorption. It has also been reported in the literature that polyacrylic acid possesses numerous carboxyl functional groups with a high tendency to bond Pb ions via complexation (chelation) reactions. He et al. [30], for example, suggested that the chelation is the dominating adsorption mechanism for lead(II) ions by a PAA/B composite. Miyajima et al. [48] also showed that Pb forms monodentate and bidentate complexes with polyacrylic acid.

Increasing Pb concentration from 400 to 800 mg L^{-1} increased the values of initial rate "h" from 44.61 to 50.97 mg g^{-1} min^{-1} for PAA–Bent and from 1.07 to 1.79 mg g^{-1} min^{-1} for Bent (Table 3), because the initial metal ion concentration plays an important role as a driving force to overcome mass transfer resistance for metal ion transport between the solution and the surface of the adsorbent [34]. The amount of Pb sorbed at equilibrium (q_e) was also found to follow the same trend. The q_e value increased from 52.33 to 81.58 mg g^{-1} for PAA–Bent and from 33.51 to 57.08 mg g^{-1} for Bent, with doubling the initial Pb concentration from 400 to 800 mg L^{-1}. There was a decrease in the rate constant k_2 for PAA–Bent and Bent when increasing the initial Pb concentration from 400 to 800 mg L^{-1} (Table 3), confirming that the solution with lower Pb concentration reaches equilibrium faster [49].

For Pb sorption on Bent, the best fit of experimental data was obtained by the Elovich model, according to the R^2 values presented in Table 3. This equation assumes that the active sites of the sorbent are heterogeneous in nature and therefore exhibit different activation energies for chemisorption [19]. The constant α increased but the constant β decreased with increasing the initial Pb concentration (Table 3), confirming the direct relationship between the Pb concentration and sorption rate as Chien and Clayton [36] showed that decrease in $1/\beta$ and/or increase in α enhance the reaction rate.

3.3. Effect of temperature on Pb sorption efficiency

Fig. 6 illustrates the effect of temperatures ranged from 15 to 50°C on Pb removal efficiency at various initial Pb concentrations. Increased Pb concentration from 50 to 1,200 mg L^{-1} resulted in decrease in percentage of Pb removal by Bent and PAA–bent at all temperatures, which can be attributed to the

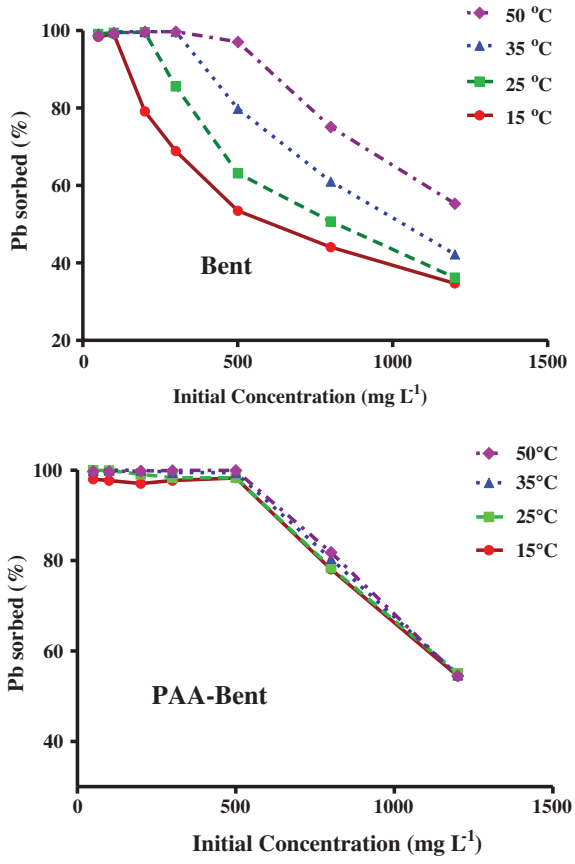

Fig. 6. Sorption percentage of Pb by the Bent and PAA–Bent at various temperatures.

saturation of available active sites on the sorbents above a certain concentration of Pb ions [50].

As can be seen from Fig. 6, the sorption percentage of Pb by Bent increased with increasing temperature. Lead sorption process was favored at higher temperatures, suggesting that the Pb sorption reaction is endothermic. This may be a result of increase in the mobility of Pb ions toward the sorbent with increasing temperature. In case of the PAA–Bent sorbent, dependence of the Pb sorption efficiency to temperature was negligible at all studied solution concentrations. It may be because of the fact that grafting of PAA on the surface and interlayer spaces of the Bent substantially increased the number of functional groups for the fast Pb complexation reactions, minimizing the effect of temperature on the overall sorption process rate.

3.4. Effect of temperature on Pb sorption isotherms

Fig. 7 shows sorption isotherms of Pb on the PAA–Bent and Bent at various temperatures. The parameters of the isotherms and correlation coefficients (R^2) are also summarized in Table 4. The sorption capacity of PAA–Bent for Pb was higher than that of Bent as deduced from the q_m values calculated for the sorbents. The K_F values of the fitted Freundlich equation also indicate that PAA–Bent has higher capacity for Pb sorption compared to the Bent (Table 4). The hybrid sorbent had also a higher affinity toward Pb ions as estimated from the greater K_L value calculated for PAA–Bent compared to Bent. The R_L values at different temperatures were all below 1.0 (Table 4), which means the adsorption is favorable [16]. Moreover, R_L values decrease with increasing temperatures, demonstrating that the ongoing adsorption process is much more favorable at higher temperatures. Similar results were also reported by Shirvani et al. [51] who studied the adsorption of Ni ions by Ca–bentonite. Considering the Freundlich N parameters represented in Table 4 also indicates that PAA–Bent binds Pb more strongly than Bent do, as smaller values of N shows stronger bonds for that specific sorbate with the surface [52].

The experimental sorption capacities varied from 56.93 to 90.48 mg g^{-1} for Bent and from 89.33 to 95.63 mg g^{-1} for PAA–Bent, depending on the temperatures. A similar trend was also observed for the q_m and K_F values calculated from the Langmuir and Freundlich equations, respectively. The increase in sorption capacities with temperature indicates the endothermic nature of the Pb sorption processes. The Langmuir affinity constant, K_L, also increased from 0.009 to 1.191 L mg^{-1} for Bent and from 0.120 to 2.249 L mg^{-1} for PAA–Bent with increasing temperature. The Freundlich N values decrease with increasing temperature, suggesting that Pb binding strength to the surface functional groups was enhanced at higher temperatures.

The equilibrium pH values of the supernatants after Pb sorption were 5.23–7.41 for Bent/Pb and from 4.87 to 6.19 for PAA–Bent/Pb systems at various concentrations from 50 to 1,200 mg L^{-1}. In fact, the final pH of the solution decreased gradually with increasing initial concentration of Pb(II). PAA–Bent composite has lots of –COOH functional groups, which can be dissociated and released protons while bonding the Pb(II) ions [7,8,27–29].

3.5. Lead sorption thermodynamics

Thermodynamic parameters of Pb sorption by Bent and PAA–Bent obtained from $\ln K_d$ vs. $1/T$ plots (Fig. 8) are given in Table 5. The negative values of ΔG° at different temperatures imply the spontaneous nature of the Pb sorption process. Further, the decrease in the values of ΔG° with the increasing

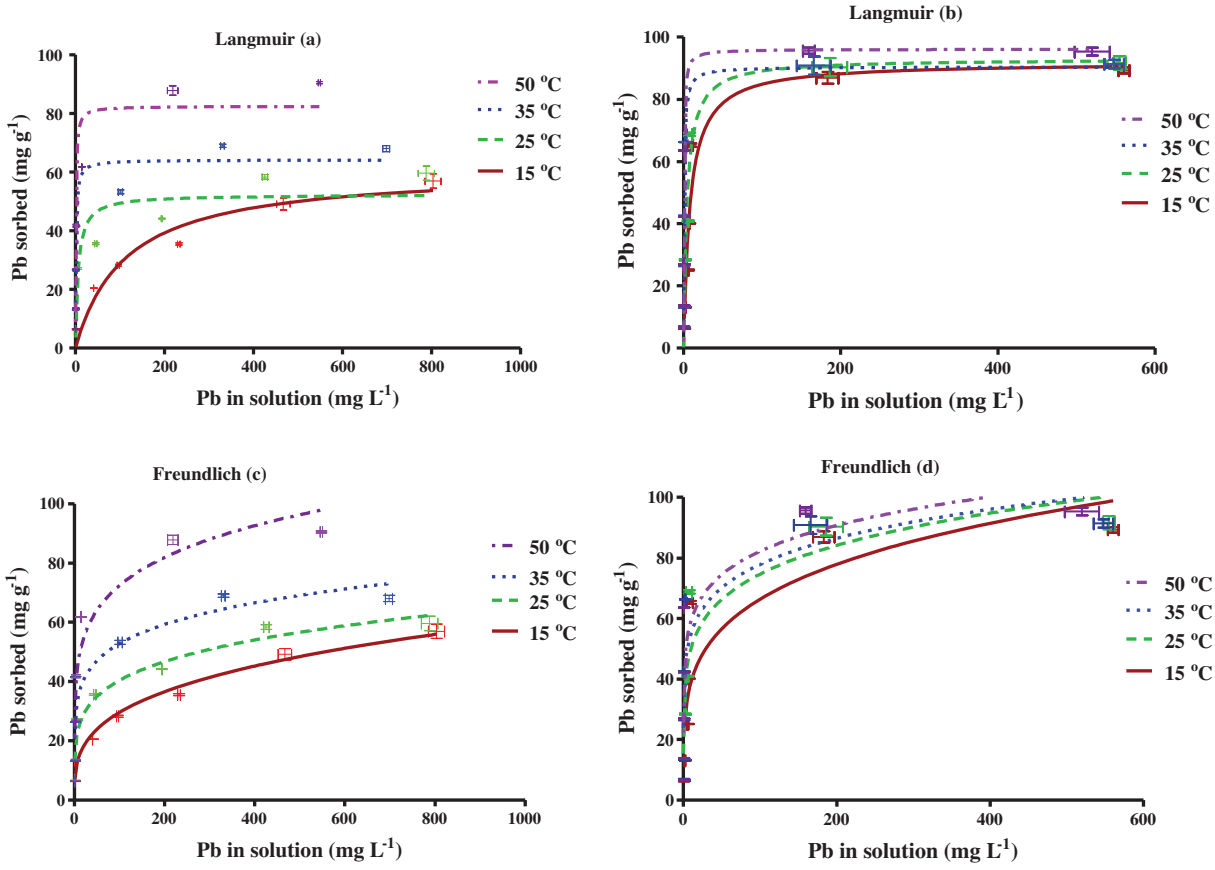

Fig. 7. Langmuir and Freundlich isotherm models fitted to equilibrium Pb sorption data onto Bent (a and c) and PAA–Bent (b and d) at different temperatures.

Table 4
Isothermal parameters and correlation coefficients calculated for Langmuir and Freundlich models fitted to the Pb sorption data on the PAA–Bent and Bent at different temperatures

	PAA-Bent				Bent			
Isothermal constants	15 °C	25 °C	35 °C	50 °C	15 °C	25 °C	35 °C	50 °C
$q_{m(exp.)}$ (mg g^{-1})	89.33	90.71	90.85	95.63	56.93	59.62	68.02	90.48
$q_{m(exp.)}$ (mmol g^{-1})	0.431	0.437	0.438	0.461	0.274	0.287	0.328	0.436
Langmuir								
q_m (mg g^{-1})	91.88	93.01	90.45	96.13	61.15	52.31	64.16	82.51
K_L (L mg^{-1})	0.120	0.226	1.456	2.249	0.009	0.168	0.873	1.191
R^2	0.921	0.943	0.981	0.947	0.871	0.862	0.928	0.943
R_L	0.148	0.080	0.013	0.008	0.700	0.105	0.023	0.016
Freundlich								
K_F	22.89	33.77	38.83	42.65	7.22	15.39	24.43	32.09
N	0.231	0.172	0.151	0.142	0.306	0.209	0.167	0.176
R^2	0.782	0.897	0.845	0.849	0.969	0.963	0.859	0.908

Notes: $q_{m(exp.)}$ is the experimentally measured maximum Pb sorption by the sorbents under the conditions applied in this experiment given to compare with the q_m values estimated by the Langmuir model.

Table 5
Thermodynamic parameters for Pb sorption onto the PAA–Bent and Bent

Sorbent	ΔS° (J mol^{-1} K^{-1})	ΔH° (kJ mol^{-1})	ΔG° (kJ mol^{-1})				R^2
			15℃	25℃	35℃	50℃	
PAA-Bent	578.42	146.359	–20.068	–26.717	–31.445	–40.629	0.995
Bent	310.94	70.023	–19.513	–22.801	–25.746	–30.447	0.999

temperature indicates the sorption was more spontaneous and favorable at higher temperatures [53,54]. Cations are readily desolvated at high temperatures, and hence their sorption becomes more favorable [54]. The values of ΔG° ranged from −20.06 to −40.62 kJ mol^{-1}, suggesting that a surface complexation reaction is the major mechanism responsible for the Pb sorption process [53,55]. PAA–Bent shows more negative values of ΔG° for Pb sorption compared to the Bent, indicating the greater affinity for Pb removal. Özcan et al. [15] also reported that ΔG° values for Pb sorption on 8-hydroxyquinoline-immobilized bentonite changed from –24.30 to –29.72 kJ mol^{-1} with increasing temperature from 20 to 50℃.

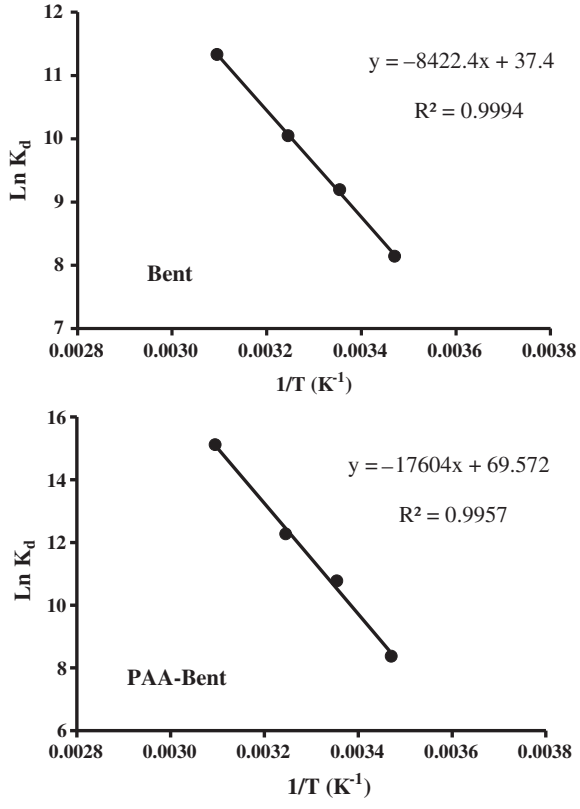

Fig. 8. Plots of ln K_d vs. $1/T$ for the estimating of thermodynamic parameters of Pb sorption by PAA–Bent and Bent.

The positive values of ΔH° (Table 5) indicate the endothermic behavior of the Pb sorption process. This fact was also demonstrated from the increase in Pb sorption with temperature (Table 4). The magnitude of ΔH° gives an idea about whether the sorption is physical or chemical in nature. The ΔH° value for physical adsorption is usually no more than 4.2 kJ mol^{-1} and for chemical adsorption is more than 21 kJ mol^{-1} [34]. Therefore, it seems that adsorption of Pb ions on PAA–Bent and Bent is a chemical process and strong interactions between the Pb ions and functional groups on the surface of PAA–Bent and Bent might be formed [34]. The greater ΔH° value was calculated for the Pb sorption process on PAA–Bent compared to the Bent which may be due to the larger activation energy of the sorption onto the PAA–Bent [23].

The positive values of ΔS° (Table 5) suggests some structural changes in the sorbents [23] and increased randomness at the solid/solution interface during the adsorption of Pb onto sorbents [53]. Chemisorption reactions are associated with decreasing the number of water molecules surrounding the sorptive ions via partial dehydration process which cause the degree of freedom of the water molecule to be increased [53,56]. The ΔS° value of the Pb sorption on PAA–Bent is higher than that on the Bent, which can be explained by the greater interactions between Pb ions and PAA functional groups on the surface of PAA–Bent nanocomposite [23].

4. Conclusions

Batch experiments indicated that poly(acrylic acid)–bentonite (PAA–Bent) hybrid sorbent is superior to bentonite (Bent) in removing of Pb from aqueous solution. Maximum sorption capacity of the hybrid sorbent at standard temperature (25℃) was found to be 90.7 mg g^{-1} which is far greater than that of natural Bent (59.6 mg g^{-1}). The capacity and affinity of both Bent and PAA–Bent for Pb sorption increased with increasing temperature. Sorption process of Pb on the PAA–Bent was fast, approaching to equilibrium within a few hours, while no distinct equilibrium condition was observed for Pb sorption on the Bent even after 1,440 min of exposure. Thermodynamic

studies showed that sorption of Pb on both Bent and PAA–Bent were endothermic and spontaneous. Overall, PAA–Bent hybrid is a potential sorbent for Pb removal from contaminated waters.

References

[1] O.A. Ogunseitan, Public health and environmental benefits of adopting lead-free solders, JOM 59 (2007) 12–17.

[2] N. Milovantseva, O.A. Ogunseitan, in: J. Nriagu, Encyclopedia of Environmental Health, Elsevier, Oxford, England, 2011, pp. 813–821.

[3] P.B. Tchounwou, C.G. Yedjou, A.K. Patlolla, D.J. Sutton, in: A. Luch, Molecular, Clinical and Environmental Toxicology, Springer Basel, Basel, 2012, pp. 133–164.

[4] CDC, Low Level Lead Exposure Harms Children: A Renewed Call For Primary Prevention, Report of the Advisory Committee on Childhood Lead Poisoning Prevention of the Centers for Disease Control and Prevention, US Department of Health and Human Services, Atlanta, GA, 2012.

[5] B. Phalguni, S. De, in: K. Mohanty, M.K. Purkait, Membrane Technologies and Applications, CRC Press, Boca Raton, FL, 2012, pp. 133–146.

[6] E. Worch, Adsorption Technology in Water Treatment: Fundamentals, Processes, and Modeling, Walter de Gruyter GmbH & Co. KG, Berlin, Germany, 2012.

[7] X. Wang, Y. Zheng, A. Wang, Fast removal of copper ions from aqueous solution by chitosan-g-poly(acrylic acid)/attapulgite composites, J. Hazard. Mater. 168 (2009) 970–977.

[8] Y. Liu, W. Wang, A. Wang, Adsorption of lead ions from aqueous solution by using carboxymethyl cellulose-g-poly (acrylic acid)/attapulgite hydrogel composites, Desalination 259 (2010) 258–264.

[9] H. Zhang, Z. Tong, T. Wei, Y. Tang, Sorption characteristics of Pb(II) on alkaline Ca-bentonite, Appl. Clay Sci. 65–66 (2012) 21–23.

[10] Q. Fan, Z. Li, H. Zhao, Z. Jia, J. Xu, W. Wu, Adsorption of Pb(II) on palygorskite from aqueous solution: Effects of pH, ionic strength and temperature, Appl. Clay Sci. 45 (2009) 111–116.

[11] M. Jiang, Q. Wang, X. Jin, Z. Chen, Removal of Pb(II) from aqueous solution using modified and unmodified kaolinite clay, J. Hazard. Mater. 170 (2009) 332–339.

[12] F. Yu, Y. Wu, J. Ma, C. Zhang, Adsorption of lead on multi-walled carbon nanotubes with different outer diameters and oxygen contents: Kinetics, isotherms and thermodynamics, J. Environ. Sci. 25 (2013) 195–203.

[13] X. Liang, Y. Xu, G. Sun, L. Wang, Y. Sun, Y. Sun, X. Qin, Preparation and characterization of mercapto functionalized sepiolite and their application for sorption of lead and cadmium, Chem. Eng. J. 174 (2011) 436–444.

[14] S.A. Kim, S.K. Kannan, K.J. Lee, Y.J. Park, P.J. Shea, W.H. Lee, H.M. Kim, B.T. Oh, Removal of Pb(II) from aqueous solution by a zeolite–nanoscale zero-valent iron composite, Chem. Eng. J. 217 (2013) 54–60.

[15] A.S. Özcan, O. Gök, A. Özcan, Adsorption of lead(II) ions onto 8-hydroxy quinoline-immobilized bentonite, J. Hazard. Mater. 161 (2009) 499–509.

[16] Y. Chang, H. Liu, F. Zha, H. Chen, X. Ren, Z. Lei, Adsorption of Pb(II) by N-methylimidazole modified palygorskite, Chem. Eng. J. 167 (2011) 183–189.

[17] V.K. Gupta, A. Rastogi, Biosorption of lead from aqueous solutions by green algae Spirogyra species: Kinetics and equilibrium studies, J. Hazard. Mater. 152(1) (2008) 407–414.

[18] E. Malkoc, Ni(II) removal from aqueous solutions using cone biomass of *Thuja orientalis*, J. Hazard. Mater. 137 (2006) 899–908.

[19] G.J. Copello, L.E. Diaz, V.C. DallOrto, Adsorption of Cd(II) and Pb(II) onto a one step-synthesized polyampholyte: Kinetics and equilibrium studies, J. Hazard. Mater. 217–218 (2012) 374–381.

[20] J. Liu, Y. Ma, Y. Zhang, G. Shao, Novel negatively charged hybrids. 3. Removal of Pb^{2+} from aqueous solution using zwitterionic hybrid polymers as adsorbent, J. Hazard. Mater. 173 (2010) 438–444.

[21] G. Crini, P.-M. Badot, Application of chitosan, a natural aminopolysaccharide, for dye removal from aqueous solutions by adsorption processes using batch studies: A review of recent literature, Prog. Polym. Sci. 33 (2008) 399–447.

[22] M.M. Motsa, B.B. Mamba, J.M. Thwala, T.A.M. Msagati, Preparation, characterization, and application of polypropylene–clinoptilolite composites for the selective adsorption of lead from aqueous media, J. Colloid Interface Sci. 359 (2011) 210–219.

[23] G. Zhao, H. Zhang, Q. Fan, X. Ren, J. Li, Y. Chen, X. Wang, Sorption of copper(II) onto super-adsorbent of bentonite–polyacrylamide composites, J. Hazard. Mater 173 (2010) 661–668.

[24] B. Pan, H. Qiu, G. Nie, L. Xiao, L. Lv, W. Zhang, Q. Zhang, S. Zheng, Highly efficient removal of heavy metals by polymer-supported nanosized hydrated Fe (III) oxides: Behavior and XPS study, Water Res. 44 (2010) 815–824.

[25] F. Googerdchian, A. Moheb, R. Emadi, Lead sorption properties of nanohydroxyapatite–alginate composite adsorbents, Chem. Eng. J. 200–202 (2012) 471–479.

[26] D. Baybaş, U. Ulusoy, The use of polyacrylamide-aluminosilicate composites for thorium adsorption, Appl. Clay Sci. 51 (2011) 138–146.

[27] T. Bala, B.L.V. Prasad, M. Sastry, M.U. Kahaly, U.V. Waghmare, Interaction of different metal ions with carboxylic acid group: A quantitative study, J. Phys. Chem. A 111 (2007) 6183–6190.

[28] B.L. Rivas, E.D. Pereira, M. Palencia, J. Sánchez, Water-soluble functional polymers in conjunction with membranes to remove pollutant ions from aqueous solutions, Prog. Polym. Sci. 36 (2011) 294–322.

[29] B.L. Rivas, E.D. Pereira, I. Moreno-Villoslada, Water-soluble polymer–metal ion interactions, Prog. Polym. Sci. 28 (2003) 173–208.

[30] Y.F. He, L. Zhang, D.Z. Yan, S.L. Liu, H. Wang, H.R. Li, R.M. Wang, Poly (acrylic acid) modifying bentonite with in-situ polymerization for removing lead ions, Water Sci. Technol. 65 (1997) 1383–1391.

[31] H.R. Rafiei, M. Shirvani, O.A. Ogunseitan, Removal of lead from aqueous solutions by a poly (acrylic acid)/bentonite nanocomposite, Appl. Water Sci. doi: 10.1007/s13201-014-0228-0.
[32] J.W. Rhoades, in: C.A. Page, Methods of Soil Analysis, ASA Press, Madison, WI, 1986, pp. 149–158.
[33] M. Shirvani, H. Shariatmadari, M. Kalbasi, F. Nourbakhsh, B. Najafi, Sorption of cadmium on palygorskite, sepiolite and calcite: Equilibria and organic ligand affected kinetics, Colloids Surf., A: Physicochem. Eng. Aspects 287 (2006) 182–190.
[34] D. Ozdes, A. Gundogdu, B. Kemer, C. Duran, H.B. Senturk, M. Soylak, Removal of Pb(II) ions from aqueous solution by a waste mud from copper mine industry: Equilibrium, kinetic and thermodynamic study, J. Hazard. Mater. 166 (2009) 1480–1487.
[35] A. Sheikhhosseini, M. Shirvani, H. Shariatmadari, Competitive sorption of nickel, cadmium, zinc and copper on palygorskite and sepiolite silicate clay minerals, Geoderma 192 (2013) 249–253.
[36] S.H. Chien, W.R. Clayton, Application of Elovich equation to the kinetics of phosphate release and sorption in soils, Soil Sci. Soc. Am. J. 44 (1980) 265–268.
[37] M. Ranđelović, M. Purenović, A. Zarubica, J. Purenović, B. Matović, M. Momčilović, Synthesis of composite by application of mixed Fe, Mg (hydr)oxides coatings onto bentonite—A use for the removal of Pb(II) from water, J. Hazard. Mater. 199–200 (2012) 367–374.
[38] G. Lagaly, M. Ogawa, I. Dékány, in: F. Bergaya, B.K.G. Theng, G. Lagaly, Handbook of Clay Science, Developments in Clay Science, vol. 1, Elsevier, Amsterdam, 2013, pp. 309–377.
[39] S.M. Lee, D. Tiwari, Organo and inorgano-organo-modified clays in the remediation of aqueous solutions: An overview, Appl. Clay Sci. 59–60 (2012) 84–102.
[40] L. Wang, A. Wang, Adsorption properties of Congo Red from aqueous solution onto surfactant-modified montmorillonite, J. Hazard. Mater. 160 (2008) 173–180.
[41] N.H. Tran, G.R. Dennis, A.S. Milev, G.S.K. Kannangara, M.A. Wilson, R.N. Lamb, Interactions of sodium montmorillonite with poly(acrylic acid), J. Colloid Interface Sci. 290 (2005) 392–396.
[42] Y. Zhao, Y. Chen, M. Li, S. Zhou, A. Xue, W. Xing, Adsorption of Hg^{2+} from aqueous solution onto polyacrylamide/attapulgite, J. Hazard. Mater. 171 (2009) 640–646.
[43] M.E. Mahmoud, M.M. Osman, S.B. Ahmed, T.M. Abdel-Fattah, Improved adsorptive removal of cadmium from water by hybrid chemically and biologically carbonaceous sorbents, Chem. Eng. J. 175 (2011) 84–94.
[44] A.R. Nesic, S.J. Velickovic, D.G. Antonovic, Characterization of chitosan/montmorillonite membranes as adsorbents for Bezactiv Orange V-3R dye, J. Hazard. Mater. 209–210 (2012) 256–263.
[45] S. Bakhtiary, M. Shirvani, H. Shariatmadari, Characterization and 2,4-D adsorption of sepiolite nanofibers modified by N-cetylpyridinium cations, Microporous Mesoporous Mater. 168 (2013) 30–36.
[46] R. Koswojo, R.P. Utomo, Y.H. Ju, A. Ayucitra, F.E. Soetaredjo, J. Sunarso, S. Ismadji, Acid Green 25 removal from wastewater by organo-bentonite from Pacitan, Appl. Clay Sci. 48 (2010) 81–86.
[47] X. Li, W. Zheng, D. Wang, Q. Yang, J. Cao, X. Yue, T. Shen, G. Zeng, Removal of Pb (II) from aqueous solutions by adsorption onto modified areca waste: Kinetic and thermodynamic studies, Desalination 258 (2010) 148–153.
[48] T. Miyajima, M. Mori, S.I. Ishiguro, Analysis of complexation equilibria of polyacrylic acid by a donnan-based concept, J. Colloid Interface Sci. 187 (1997) 259–266.
[49] Y. Wang, X. Tang, Y. Chen, L. Zhan, Z. Li, Q. Tang, Adsorption behavior and mechanism of Cd(II) on loess soil from China, J. Hazard. Mater. 172 (2009) 30–37.
[50] P.S. Kumar, S. Ramalingam, S.D. Kirupha, A. Murugesan, T. Vidhyadevi, S. Sivanesan, Adsorption behavior of nickel(II) onto cashew nut shell: Equilibrium, thermodynamics, kinetics, mechanism and process design, Chem. Eng. J. 167 (2011) 122–131.
[51] M. Shirvani, H.R. Rafiei, S. Bakhtiary, B. Azimzadeh, S. Amani, Equilibrium, kinetic, and thermodynamic studies on nickel removal from aqueous solutions using Ca-bentonite, Desalin. Water Treat. 54 (2014) 1–9.
[52] US Environmental Protection Agency, Drinking Water Treatability Database, GAC Isotherm, US Environmental Protection Agency, Cincinnati, OH, 2009.
[53] H. Chen, A. Wang, Adsorption characteristics of Cu (II) from aqueous solution onto poly(acrylamide)/attapulgite composite, J. Hazard. Mater. 165 (2009) 223–231.
[54] S. Yang, D. Zhao, H. Zhang, S. Lu, L. Chen, X. Yu, Impact of environmental conditions on the sorption behavior of Pb(II) in Na-bentonite suspensions, J. Hazard. Mater. 183 (2010) 632–640.
[55] E. Eren, Removal of lead ions by Unye (Turkey) bentonite in iron and magnesium oxide-coated forms, J. Hazard. Mater. 165 (2009) 63–70.
[56] A. Sdiri, T. Higashi, T. Hatta, F. Jamoussi, N. Tase, Evaluating the adsorptive capacity of montmorillonitic and calcareous clays on the removal of several heavy metals in aqueous systems, Chem. Eng. J. 172 (2011) 37–46.